Developments in Soft X-Ray Spectral Modelling for Fusion: Areas of Overlap with Astrophysics

A. D. Whiteford*, N. R. Badnell*, R. Barnsley†, I. H. Coffey†,
M. G. O'Mullane*, H. P. Summers* and K.-D. Zastrow**

*Department of Physics University of Strathclyde Glasgow G4 0NG UK
†Department of Physics Queens University Belfast UK
**UKAEA Fusion Culham Science Centre Abingdon OX14 3EA UK

Abstract.
This paper focuses on the diagnostic analysis in magnetically confined fusion plasmas with attention drawn both to the methodology in common with that in astrophysics and to points of departure – such as species, transport, high density and the role of neutral hydrogen. Comment is also made on the state of high quality theoretical collision data from a fusion perspective and how it can support rigorous error analysis of better spectroscopic measurements.

Keywords: Fusion, Astrophysics, X-ray, Atomic Modelling, Error Propagation
PACS: 32.30.Rj, 32.70.-n, 52.20.Fs, 95.30.Dr, 95.85.Nv, 52.70.La

1. INTRODUCTION

Quantitative x-ray spectroscopy has a long history in astrophysics. The use of the helium-like resonance region with its associated dielectronic satellite emission as a quantitative tool was first performed extensively by [1]. Since then, analysis of this spectral feature and others in the soft x-ray has been performed exhaustively in both the astrophysical and fusion communities — sometimes with different goals but with the same common underlying atomic physics and modelling requirements. It is often the case that communication between these two communities is far from ideal.

An example of a helium-like iron spectrum, recorded on the TEXTOR[1] tokamak is shown in figure 1. This same spectrum is also seen in astrophysics (especially in the flaring solar corona — albeit with small variations of detail).

An EUV/soft x-ray spectrum of tungsten inside the JET[2] tokamak is shown in figure 2. This is a spectrum with no astrophysical parallel, although, spectra of species beyond iron (i.e. $z > 26$) have been observed, e.g. nickel in the soft x-ray[22] and elements such as tantalum (very close to tungsten on the periodic table and also routinely ablated into JET) have also been observed (although not in the x-ray) and understanding them is of considerable current interest in nuclear astrophysics.

The opportunities for the fusion community differ from that of the astrophysical community. In modern fusion devices (e.g. a tokamak), the laboratory environment

[1] Tokamak EXperiment for Technology Oriented Research, see [8]
[2] Joint European Torus, see [7]

CP774, *X-Ray Diagnostics of Astrophysical Plasmas,* edited by Randall K. Smith

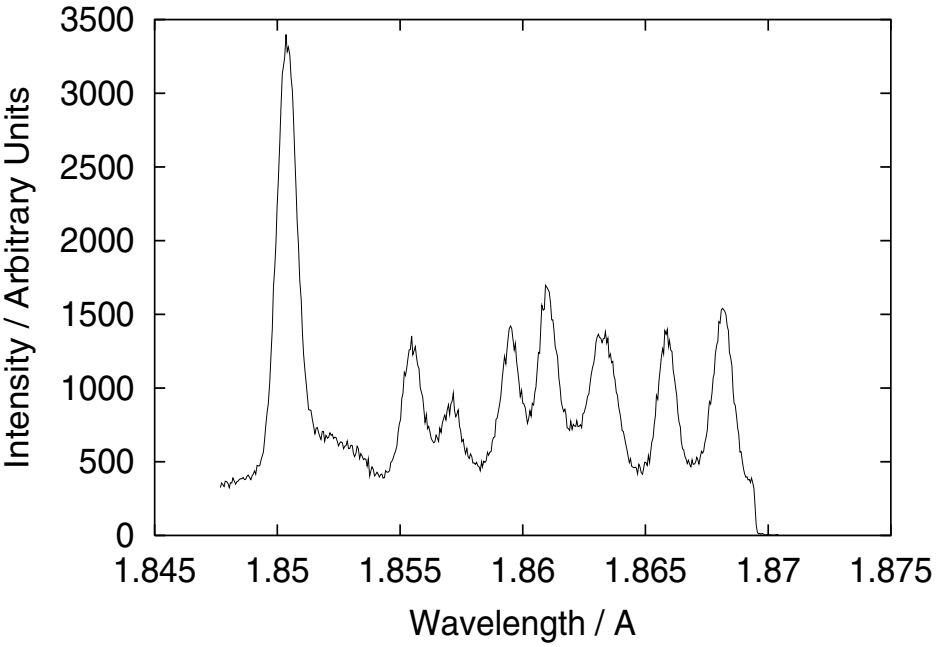

FIGURE 1. Helium-like resonance region of Fe^{24+} measured on TEXTOR in shot 15721.

for spectral measurements allows for multiple lines of sight through the plasma. Thus, for example, x-ray bolometry diagnostics can yield full tomographic reconstructions of the plasma. Also, active diagnostics play a key role in fusion analysis. Most machines have a Thomson scattering system to measure the electron temperature and density both temporally and spatially across the plasma. Although there are fewer unknowns in the modelling of the spectral emission, there is an expectation/requirement for greater accuracy. Despite the difference in applications and utilisation, the fundamental and applied atomic physics entering the modelling of soft x-ray emission are common to the two communities.

The layout of this paper is as follows: in section 2 we discuss the various methods of calculating fundamental atomic data and how they impact the modelling of emission from plasmas. In section 3 we discuss collisional–radiative modelling to provide derived atomic data suitable for direct use in plasma modelling codes and spectral analysis. In section 4 we discuss theoretical uncertainties on fundamental atomic data, comment on how to estimate them and outline the methodology used to propagate these uncertainties through to derived atomic data. Sections 2, 3 and 4 are mainly from a fusion perspective. We then finish with some short conclusions drawing attention to mutually advantageous areas of overlap between fusion and astrophysical analysis.

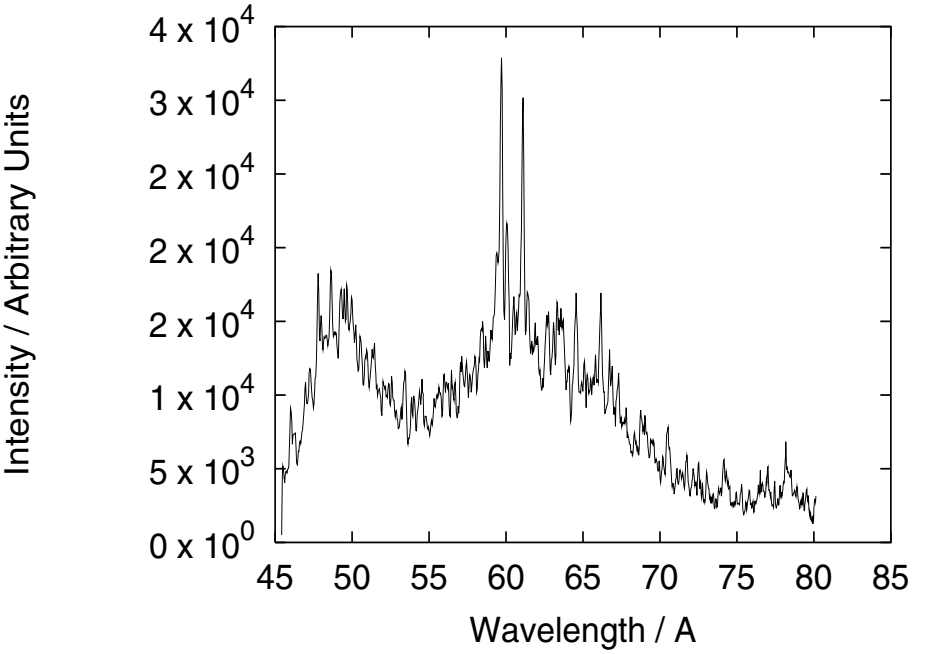

FIGURE 2. Spectrum recorded from ablation of a tungsten tile into JET using a grazing incidence spectrometer for shot 55155.

2. FUNDAMENTAL ATOMIC DATA

We distinguish three levels of fundamental atomic data, namely, baseline data, intermediate quality data and high quality data. A brief summary of methods use to calculate cross-sections is given in table 1. Key to all the methods given in table 1 is that they rely on a detailed (i.e. multi-configuration, multi-electron) atomic structure. Several codes exist to do this, such as SUPERSTRUCTURE[20], AUTOSTRUCTURE[19] and the Cowan code[21]. The possibility for quick construction of (effectively) complete atomic structures has rendered largely obsolete semi-analytical expressions such as that of [18] which are also unwarranted for precision analysis of measurements from current instrumentation. Computational advances mean that, e.g., plane wave Born calculations even for very heavy species can be performed rapidly and the quality of the atomic structure available gives a precision to the approximation which exceeds the expectations of Born.

At the high precision end of the scale, use of *R*-matrix data for the helium-like stage is now routine (see, e.g., [2], [11], [12]). However, important effects must be considered to realise the full potential of *R*-matrix. One such effect is that of radiation damping. Figure 3 shows the resonance contribution to the effective collision strength and also the reduction of this effective collision strength due to radiation damping. It can be seen that both of these effects matter — neglecting radiation damping would lead to a large overestimate of the excitation rate at low temperatures. For more details on the

TABLE 1. Summary of main cross-section determination techniques along with the major advantages and disadvantages

Type	Advantages	Disadvantages
Measurement	Real Results	Restricted energy ranges
Plane Wave Born	Quick to perform	Baseline quality results
Unitarised Born	Quick to perform	Baseline quality results
Distorted-Wave	Fairly quick	No resonances
CCC*	Valid at all energies	Slow resonance resolution
R-matrix	Rapid resonance resolution	Not valid at all energies
TDSE†	Very accurate	Very slow

* Convergent Close Coupling
† Time Dependent Schrödinger Equation

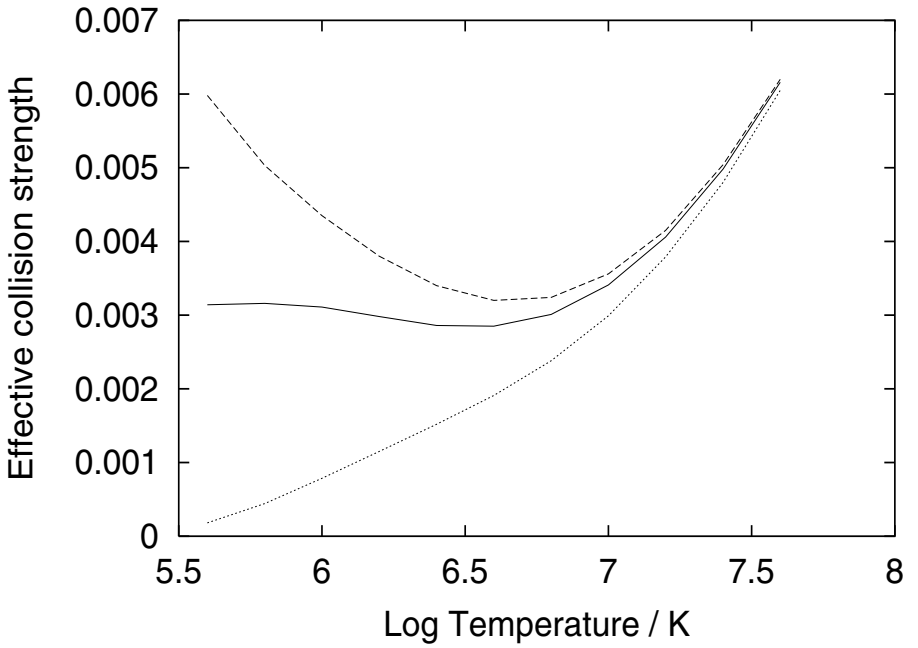

FIGURE 3. Effective collision strengths for the electron-impact excitation of the $1s2p\ ^1P_1 - 1s3s\ ^1S_0$ transition in Ar^{16+}. The solid curve denotes results that include the radiation damping of resonances. The dashed curve denotes results that omit the radiation damping of resonances. The dotted curve denotes results for the underlying (non-resonant) background only.

background to the inclusion of radiation damping with the *R*-matrix approach see [9] and for details of the calculations themselves see [2].

For the lithium-like system, calculations on the electron impact excitation requires slightly more computational effort but are still well within the scope of moderate computer systems (see [3] for examples of calculations for argon and iron). An important effect in this case is Auger damping to intermediate resonance states outside the *R*-

TABLE 2. Contributions to the effective collision strength (divided by 10^{-4}) of the $1s^2 2s\,^2S_{\frac{1}{2}} - 1s2s^2\,^2S_{\frac{1}{2}}$ transition in Fe^{23+} showing contributions with Auger damping not implicitly present in the *R*-matrix method included (ADI) and such damping excluded (ADE).

Temperature	3×10^5K		3×10^6K		3×10^7K		3×10^8K	
Contribution	ADI	ADE	ADI	ADE	ADI	ADE	ADI	ADE
Background	9.48		9.49		9.51		10.0	
1s2s2p*nl*	0.92	2.92	0.05	0.47	—*	—	—	—
1s2s3*l*3*l*′	—	—	1.41	1.41	0.49	0.49	0.01	0.01
1s2s3*l*4*l*′	—	—	0.11	0.13	0.20	0.22	0.01	0.01
1s2s3*l*5*l*′	—	—	0.09	0.09	0.24	0.26	0.01	0.01
1s2s3*nl*′†	—	0.11	—	—	0.02	0.69	—	0.01
Total	10.4	12.5	11.1	11.6	10.4	11.2	10.0	10.0

* Denotes negligible contribution

† $n \geq 6$

matrix close-coupling expansion. Table 2 shows the effects of such damping. Details of the methods used are given in [10]. The issue is also discussed in [13] where the importance of Auger damping is not only highlighted but comment is made that, with the exception of [3], all previous publications had excluded the effect.

For more complex atomic systems (principally those of iron), extensive work has been performed by the Iron Project[14] although much of the calculated data has yet to be made available publicly in a useful form for plasma modelling.

For very heavy species, fully relativistic *R*-matrix theory allows an appropriate treatment (c.f. the DARC codes[15]). A recent calculation on Ni-like xenon has been performed by [16], this ion has importance in the field of x-ray lasers and the use of high-precision data is necessary in order to accurately model measurements. The collision strength for the lasing transition is shown in figure 4.

Figure 5 outlines the number of levels which are required in a comprehensive calculation for tungsten. For the more complex ionisation stages, where *R*-matrix is not yet feasible, less accurate cross-section determination techniques are utilised (see table 1). The imperative need for modelling information on very complex species necessitates the use of simpler atomic data production techniques. The scheme used along with a discussion of targeted high-quality calculations such as those of [16] discussed above is given in section 3.

3. ATOMIC MODELLING AND KEY ATOMIC DELIVERABLES FOR FUSION

The fundamental atomic data production methods discussed in the previous section are critical for the spectroscopic analysis of both fusion and astrophysical plasmas however the completion of the collision calculation alone does not constitute a solved problem.

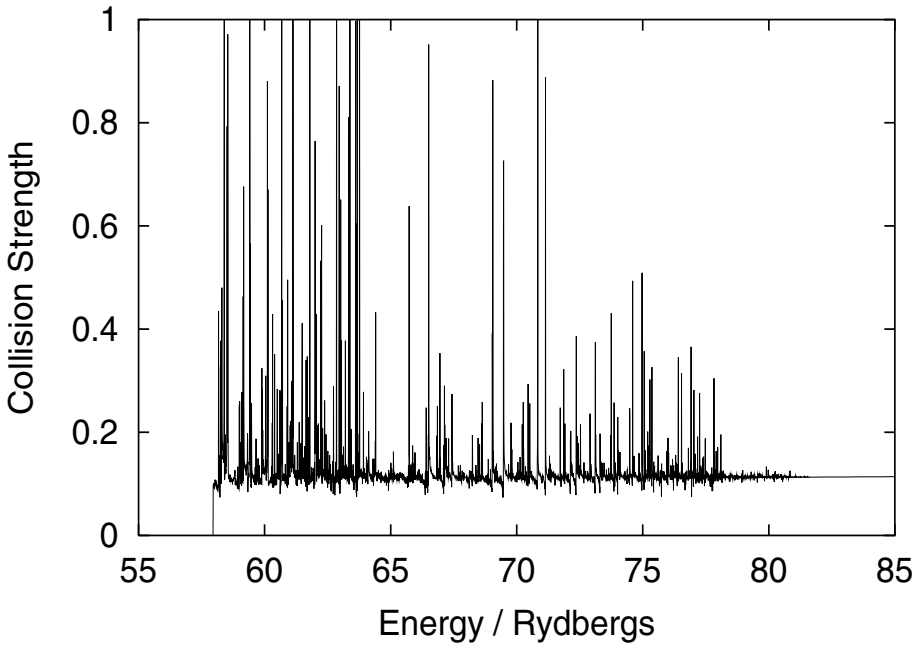

FIGURE 4. Dirac-Coloumb *R*-matrix collision strength for the $3d^{10}\,{}^1S_0 - 4d\,{}^1S_0$ transition in Xe^{26+}.

Data which originates from fundamental cross sections must be transformed into *derived atomic data* via population models. It is this latter data which is tailored to and applies to spectroscopic analysis techniques and plasma modelling. The population approach in the fusion community recognises the different plasma relaxation timescales. Specifically, we separate states of an ion into *ordinary levels* and *metastable levels*. The ordinary levels have relaxation times much faster than the timescales on which the plasma is evolving (in the fusion case, the timescales are nanoseconds versus milliseconds) so can be treated to be in quasi-equilibrium with the metastable levels. The latter may have atomic timescales similar to those of the plasma timescales. This model basis means that populations relative to metastable states can be calculated along with source terms (for transport equations) only for the metastables. These may then be archived as a function of both temperature and density. This formulation yields the key deliverables:

- Effective ionisation, recombination and power coefficients.
- Photon emissivity coefficients.

The inclusion of finite density effects along with the metastable resolution is called *generalised collisional radiative modelling*[17] in the fusion community. Such a treatment is often lacking in astrophysical analysis which assumes that the zero-density coronal picture is valid.

Turning to the quality of data required for this modelling, figure 6 shows the fractional change in ionisation potential as a function of charge in tungsten. The peaks in the

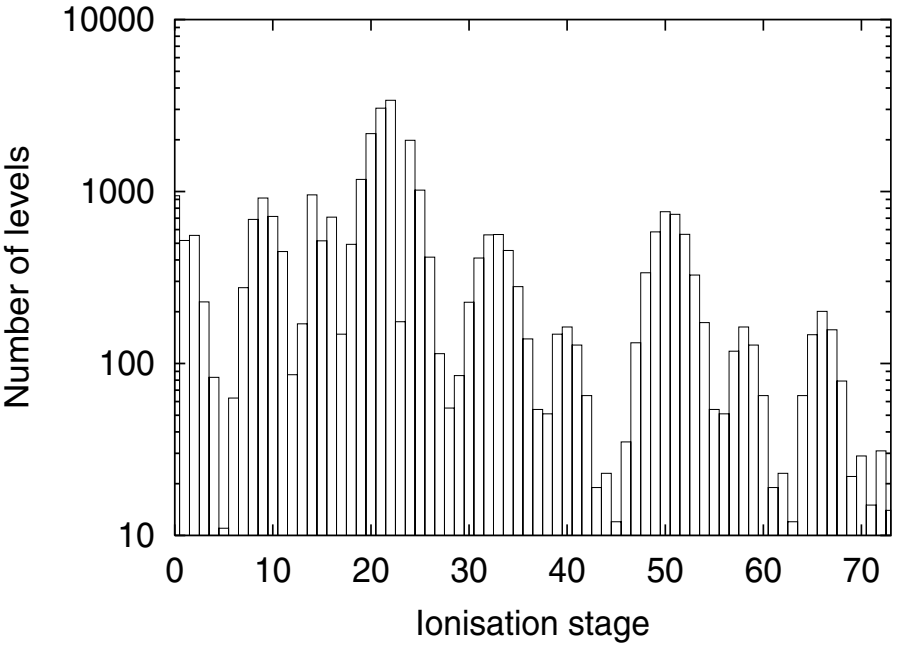

FIGURE 5. Number of levels included in tungsten excitation calculations for each ionisation stage.

curve correspond to shell boundaries and hence ions which will have extended fractional abundance in temperature space under equilibrium conditions. When interpreting spectral emission, these ions are often the ones from which spectral diagnostics arise. Hence, our approach is to use baseline cross-sections such as plane wave Born for complete coverage of a full iso-nuclear sequence (of a heavy species) and then target calculations on key ionisation stages, for more details of this approach as used for xenon see [16].

The emission from the stages not on shell boundaries for complex ions tends to have many, usually unidentifiable, lines which can even merge into a so-called *quasi-continuum*. This was exemplified in the tungsten spectrum show in figure 2. For these ions our approach is to assemble all the lines in a spectral interval (usually determined for a spectrometer detector wavelength range) so that instead of tabulating line emission as a function of temperature, density and transition we tabulate as a function of temperature, density and wavelength. We call these tabulations feature-photon-emissivity-coefficients. Such a coefficient for W^{30+} is shown in figure 7. The merging of the individual lines into a quasi-continuum also means that the atomic data used does not have to be that of the highest accuracy.

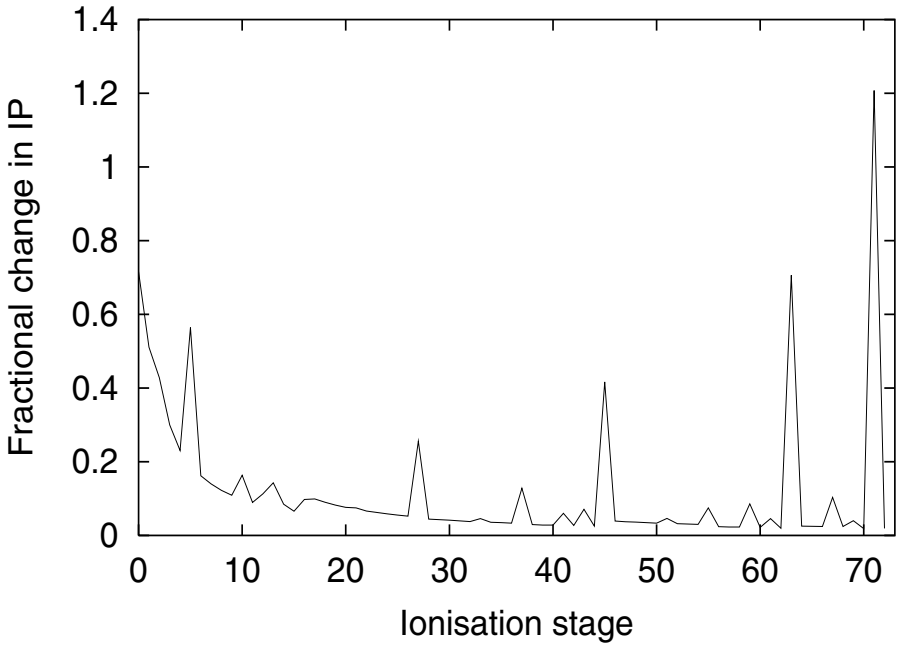

FIGURE 6. Fractional change in the ionisation potential of krypton as a function of charge state. The sharp peaks correspond to shell boundaries — see text for discussion.

4. UNCERTAINTY ESTIMATES AND ERROR PROPAGATION

The question of whether a discrepancy between a measurement and a model is due to an as yet undiscovered phenomenon, transport or inaccuracy of atomic data is one which is often asked in fusion. At issue in this confrontation is the uncertainty in the theoretical *derived* (section 3) quantities. Through the collisional-radiative and transport modelling these have a complex dependence on the uncertainties in the *fundamental* (section 2) atomic data.

Estimation of the uncertainties on theoretical cross-sections is necessary. Without such estimations it is not possible to draw firm conclusions on many results, both in astrophysical and fusion plasmas. Estimations of uncertainty in theoretical atomic data are seldom published and, if they are, then in vague generalisations rather than as tabulations on a point-by-point basis along with the calculated values. Such a practice would be almost unthinkable in the corresponding experiments to measure cross sections.

Our approach to uncertainties in the derived data is to start with a basis set of uncertainties in the fundamental atomic data[3] and then to process them through a finite-density collisional-radiative model (see section 3) using Monte-Carlo sampling. An

[3] As discussed, this basis set is never as comprehensive or precise as it should be.

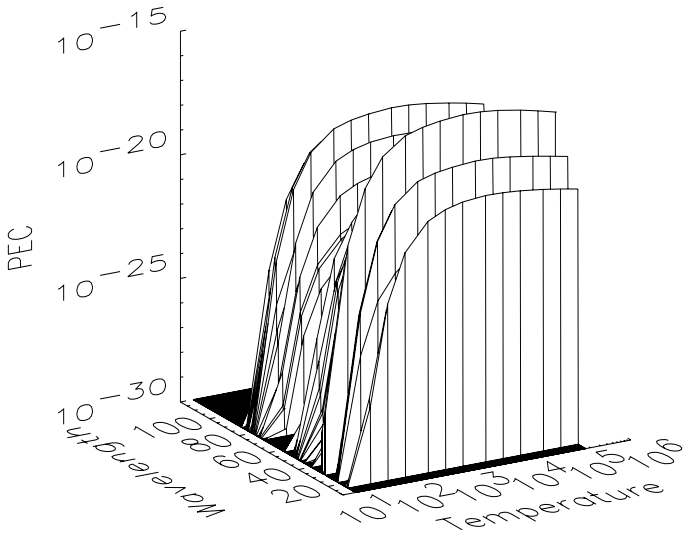

FIGURE 7. Feature-photon-emissivity coefficent for W^{30+} at an electron density of $10^{14}cm^{-3}$.

implementation of this procedure[5] (extended to include dominant error analysis as well as composite error analysis) has been successfully applied to He[6] and Fe^{24+}[2]. A more detailed overview is given in [4].

Results for Fe^{24+} are shown here in illustration, where for simplicity we assumed 10% Gaussian uncertainties on all transitions (for a discussion of the effects of taking different uncertainties for different transitions see [6] and [2]). 3000 separate collisional-radiative calculations using Monte-Carlo sampling from the fundamental atomic data were performed.

Figure 8 shows the distribution of results for the population of the 1s2s $^3S_1$ level in Fe^{24+} along with a Gaussian fitted to the results. Experience has shown that in most cases, non-linearity is not an issue in the simple excitation case; Gaussian uncertainties in the collision strengths lead to Gaussian uncertainties in the populations (hence emission)[4].

Figure 9 shows the width of the fitted Gaussian (i.e. the percentage error) as a function of density. The coronal extreme where only one excitation rate matters can be clearly seen at low density along with the LTE regime where the individual excitation rates are of no importance. The finite-density collisional-radiative regime clearly shows the need for advanced error propagation such as the method described here.

[4] We note that non-linearity can affect other processes such as beam stopping.

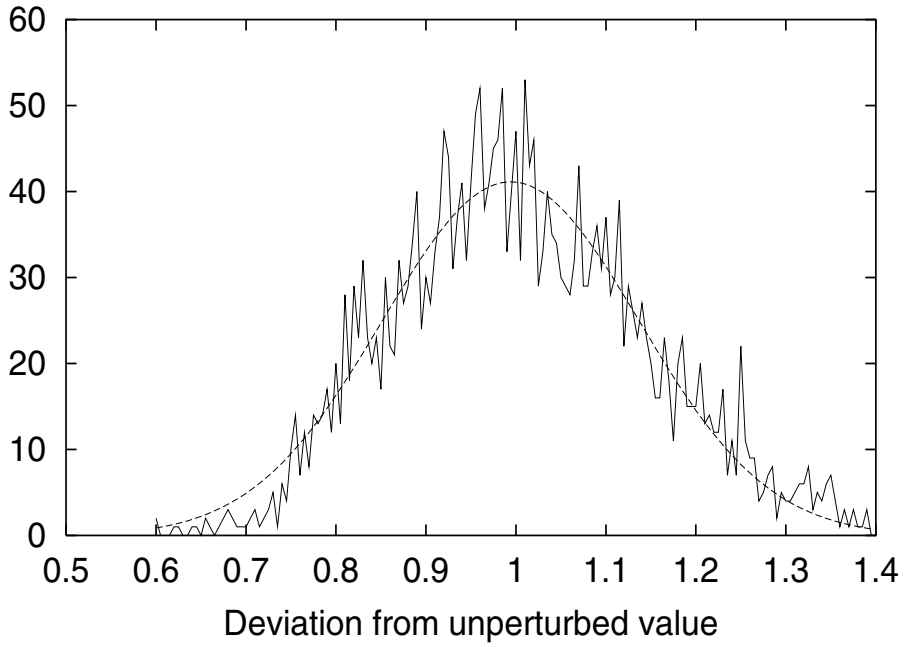

FIGURE 8. Monte-Carlo distribution of the population of the 1s2s $^3S_1$ level in Fe^{24+} assuming 10% error in all rates.

5. OVERLAPS WITH ASTROPHYSICAL ANALYSIS AND CONCLUSIONS

Shared interest in the production of electron-collisional data is a strong area of overlap between the fusion and astrophysical communities. Such data is best calculated iso-electronically as this gives the strongest check at the production phase. The two communities have different interests in which ions they require data for, however, both communities should strive for coverage along an iso-electronic sequence allowing the data to be validated in the two, often very different, scientific environments.

Finite-density effects and dynamic transport modelling are essential in the fusion domain but also impact the astrophysical regime, perhaps more than it is generally considered or implemented within the spectroscopic modelling codes available.

Shared interest in estimation of uncertainties of the fundamental atomic data is clear; it is essential in the application of models. This is not an easy task for the fundamental calculations and systematic error as well as uncertainty should always be considered. Nevertheless, the calculator generally has in his mind supplementary checks to establish the uncertainty status of their results. It is important for the user community to have these uncertainty estimates written down rather than to read a plethora of papers simply identifying discrepancies between calculations.

The area of ion-impact data and, in particular the charge exchange process, has a key

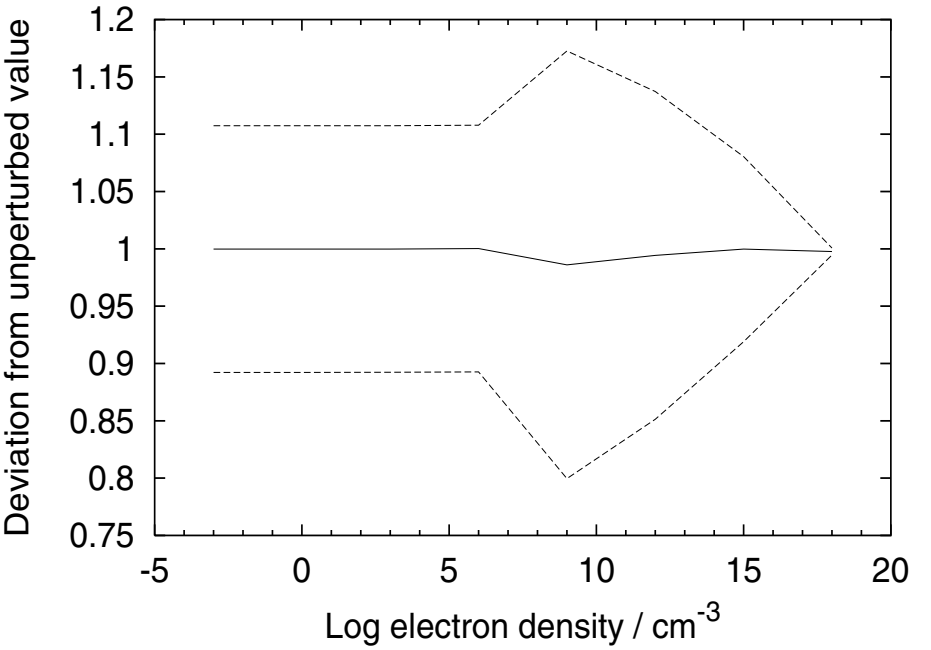

FIGURE 9. Propagated uncertainty to the population of the 1s2s $^3S_1$ level in Fe^{24+} assuming 10% error in all rates. Note the progression of the errors from the coronal, through collisional-radiative, to LTE regime.

role in the fusion community and is also being considered in astrophysics in shocks and the interaction of the solar wind with cometary atmospheres. However, there seems to be little in the way of communication (certainly much less than in the electron-impact case) on this topic. Both communities would be enhanced through comparisons of data, methods and results.

ACKNOWLEDGMENTS

ADW acknowledges an invitation and funding to attend the XDAP meeting from the Harvard-Smithsonian Center for Astrophysics. The work presented here is funded by the ADAS Project.

REFERENCES

1. A H Gabriel *Mon. Not. R. Astr. Soc.* **160** 99–119 (1972)
2. A D Whiteford, N R Badnell, C P Ballance, M G O'Mullane, H P Summers and A L Thomas *J. Phys. B: At. Mol. Opt. Phys.* **34** 3179–3191 (2001)
3. A D Whiteford, N R Badnell, C P Ballance, S D Loch, M G O'Mullane and H P Summers *J. Phys. B: At. Mol. Opt. Phys.* **35** 3729–3740 (2002)

4. H P Summers, N R Badnell, M G O'Mullane, A D Whiteford, R Bingham, B J Kellett, J Lang, K H Behringer, U Fantz, K-D Zastrow, S D Loch, M S Pindzola, D C Griffin and C P Ballance *Plasma Phys. Control. Fusion* **44** B323–B338 (2002)
5. ADAS User Manual Program: ADAS216 `http://adas.phys.strath.ac.uk`
6. Y Andrew and M G O'Mullane *Plasma Phys. Control. Fusion* **42** 301–307 (2000)
7. `http://www.jet.efda.org/`
8. `http://www.fz-juelich.de/ipp/textor_en/`
9. Robicheaux F, Gorczyca T W, Pindzola M S and Badnell N R *Phys. Rev. A* **52** 1319–33 (1995)
10. Gorczyca T W and Robicheaux F *Phys. Rev. A* **60** 1216–25 (1999)
11. F Delaheye and A K Pradhan *J. Phys. B: At. Mol. Opt. Phys.* **35** 3377–3390 (2002)
12. M A Bautista *J. Phys. B: At. Mol. Opt. Phys.* **36** 1503–1514 (2003)
13. M A Bautista, C Mendoza, T R Kallman and P Palmeri *Astronomy and Astrophysics* **403** 339–355 (2003)
14. D G Hummer, K A Berrington, W Eissner, A K Pradhan, H E Saraph and J A Tully *Astronomy and Astrophysics* **279** 298–309 (1993)
15. P H Norrington and I P Grant *J. Phys. B: At. Mol. Opt. Phys.* **20** 4869–81 (1987)
16. N R Badnell, K A Berrington, H P Summers, M G O'Mullane, A D Whiteford and C P Ballance *J. Phys. B: At. Mol. Opt. Phys.* **37** 4589–4601 (2004)
17. H P Summers and M B Hooper *Plasma Physics* **25** 1311–1344 (1983)
18. van Regemorter H *Astrophys. J.* **136** 906–15 (1962)
19. Badnell N R *J. Phys. B: At. Mol. Opt. Phys.* **30** 1–11 (1997)
20. Eissner W, Jones M and Nussbaumer H *Comput. Phys. Commun.* **4** 270–306 (1974)
21. Cowan R D *The Theory of Atomic Structure and Spectra* (Berkeley: University of California Press) (1981)
22. S Molendi, S Bianchi and G Matt *Mon. Not. R. Astr. Soc.* **343** 1 (2003)